IEEE Access
Multidisciplinary | Rapid Review | Open Access Journal

Received 7 December 2023, accepted 27 December 2023, date of publication 4 January 2024, date of current version 29 February 2024.

Digital Object Identifier 10.1109/ACCESS.2024.3349945

RESEARCH ARTICLE

Mechanical Modeling of Oil-Immersed Louver Contacts on the Valve Side of a Converter Transformer

ZHICHENG HUANG[1,2], FAN LIU[1,2], YANMING TU[1,2], JIAHUI CHEN[1,2], SHIHONG HU[1,2], TAO ZHAO[3], (Member, IEEE), AND YUNPENG LIU[3], (Member, IEEE)

[1]State Grid Sichuan Electric Power Research Institute, Chengdu 610000, China
[2]Power Internet of Things Key Laboratory of Sichuan Province, Chengdu 610000, China
[3]Hebei Provincial Key Laboratory of Power Transmission Equipment Security Defense, North China Electric Power University, Baoding 071003, China

Corresponding author: Zhicheng Huang (HXC20170113@163.com)

This work was supported in part by the Science and Technology Project of State Grid Sichuan Electric Power Company under Grant 52199722000U.

ABSTRACT Degradation of the mechanical properties of oil-immersed louver contacts is an important cause of exceeding the DC resistance on the valve side of extra-high voltage converter transformers. In this paper, the mapping relationship between force-deformation and force-contact resistance of oil-immersed louver contacts is measured and obtained by utilizing the performance test platform of oil-immersed louver contacts. Based on the stress-strain curves of the stainless steel of the strap under different temperature conditions, a mechanical simulation model of the oil-immersed louver contacts was established. Based on this model, the effects of the plastic deformation temperature of the louver contacts and the stainless steel keel structure on the heating power of the strap are investigated. The results show that the mechanical properties of the louver contacts decrease with the increase in temperature, and the permanent plastic deformation of the strap occurs when the operating temperature reaches 400 °C. Appropriately increasing the torsion angle and thickness of the stainless steel keel can slow down the local overheating of the louver contacts caused by eccentricity. The research results are helpful to understand the mechanism of local overheating failure of oil-immersed electric contact parts, and provide a reference for the design, fault analysis and further research of oil-immersed electric contact parts.

INDEX TERMS Oil-immersed louver contacts, mechanical modeling, overheating failure, structural optimization.

I. INTRODUCTION

Oil-immersed louver contacts are the key connectors for realizing the temperature compensation and current-carrying of valve-side bushings of extra-high voltage converter transformers. Since 2021, several extra-high voltage converter stations of the State Grid of China have experienced exceeding valve-side direct resistance of converter transformers due to the deterioration and failure of oil-immersed louver contacts, which causes abnormal heating of valve-side bushings and malignant failures such as flashover or even explosions, and seriously threatens the safe operation of the power system [1], [2]. At present, there are more than 1300 valve-side bushings in the converter stations of UHV DC projects in operation in China, which realize large current transmission with the converter transformer through the oil-immersed louver contacts, and the degradation of the performance of the electrical connection components with the increase of the operation time constitutes a serious safety hazard in the UHV transmission projects [3], [4], [5], [6].

Field inspection found that mechanical properties degradation (plastic deformation), wear in the electrical contact area and corrosion of silver-plated copper contact pieces are the most important degradation characteristics of the louver contacts after long-term service. The connection structure of louver contacts on the valve side of the UHV converter transformer and the morphology and characteristics of the deteriorated contact pieces are shown in Fig. 1.

The associate editor coordinating the review of this manuscript and approving it for publication was Inam Nutkani.

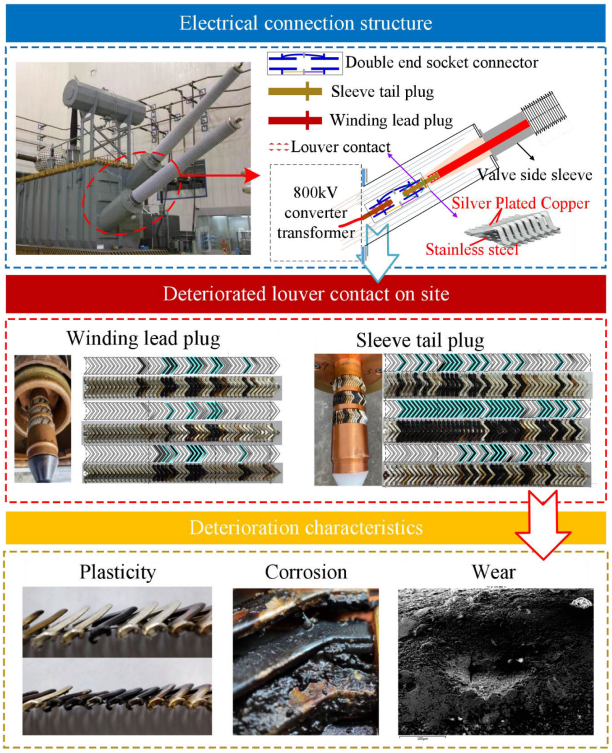

FIGURE 1. The connection structure of louver contacts on the valve side of the UHV converter transformer and the morphology and characteristics of the deteriorated contact pieces.

In Fig. 1, each faulty oil-immersed louver contacts consists of 47 silver-plated copper contacts crimped with a spring stainless steel skeleton. Among them, the stainless steel skeleton of the louver contacts plays a mechanical support role, so that the silver-plated copper contact sheet maintains a comparable current-carrying contact area with the outer wall of the plug and the inner wall of the sleeve under the action of elastic force, forming a good conductive path. In operation, a total of 141 touch pieces of three louver contacts are connected in parallel with copper plugs and inserts to achieve large current transmission. In the figure, some of the contact pieces on the deteriorated strap have collapsed and lost their elasticity, and the phenomenon will lead to a decrease in the contact force of the contact pieces or even a false connection, resulting in the exceeding of the direct resistance on the valve side of the converter transformer. At present, scholars have completed stage-by-stage research on the deterioration of electrical contacts on the strap in terms of failure mechanism, electro-thermal analysis, corrosion and wear laws. In terms of failure mechanism, Zhou et al. [5] analyzed the microstructure and elemental composition of the surface of the deteriorated contact piece based on the SEM-EDS inspection results, and the results showed that the thermal expansion and contraction of the material due to the change of the load current would cause the mechanical wear of the contact piece, mechanical wear of the contact piece, and corrosion was the main cause of the failure of the louver contact. Duan [1] found, based on the results of thermal resistance test, SEM-EDS, and XRD, that the uneven distribution of the contact resistance of the louver contacts caused by the eccentricity of the plugs and sockets led to the localized overheating of the strap, which triggered the corrosion and deterioration of the contact pieces, resulting in the contact failure of the strap. In terms of electro-thermal analysis, Gatzsche and Michael [7] established a comprehensive electro-thermal analysis method for gas-insulated sleeves. The results show that localized hot spots occur in the spring strap at the copper-aluminum joints under high-current operating conditions and progressively develop into insulation failures.

Gatzsche et al. [8], [9] experimentally investigated the applicability of the potential-temperature relationship to high-current electrical contact systems, and the results show that when the effect of ambient heat dissipation is more pronounced, the V-T relationship of the electrical contact system deviates, but it can still be used to efficiently assess the contact piece's maximum temperature rise. In terms of corrosion and wear, Jin et al. [10], [11] investigated the corrosion characteristics of louver contacts under gas insulation conditions, and the results showed that the contact resistance of the contact pieces increased by about 14% due to the fluoride generated from the copper substrate and SF6 after the contact pieces were worn out, and the wear characteristics of the high-voltage GIS plug-in current-carrying structure were investigated by Guo and Chen [12], and the results showed that the contact resistance of the louver contacts decreased with the increase of pressure, and decreased with the increase of pressure, and decreased with the increase of pressure. pressure increases, and the fluctuation of contact resistance of the contact piece decreases and then increases with the increase of the number of abrasions. In fact, in addition to corrosion and wear, the elastic force applied to the contact piece also determines the contact resistance of the contact piece to a large extent, but the existing research lacks the exploration of the degradation of the mechanical properties of the louver contact, which is a key deterioration characteristic.

In this paper, the performance test platform of louver contacts was used to obtain the mapping relationship between force-deformation and force-contact resistance of contact pieces. Based on the measured stress-strain curves of the strap stainless steel at different temperatures, a mechanical simulation model of the oil-immersed louver contact was established to investigate the plastic deformation temperature of the louver contact as well as the influence of the stainless steel keel structure on the heating power under the eccentricity condition. The conclusions obtained can provide a reference for the design, failure analysis and further research of oil-immersed electric contact parts.

II. EXPERIMENT

A. EXPERIMENTAL PLATFORM

Fig. 2 illustrates a mechanical property test platform for a louver contact. The platform consists of the fixed end, indenter, pressure sensor, fixture, slide, micrometer, slider,

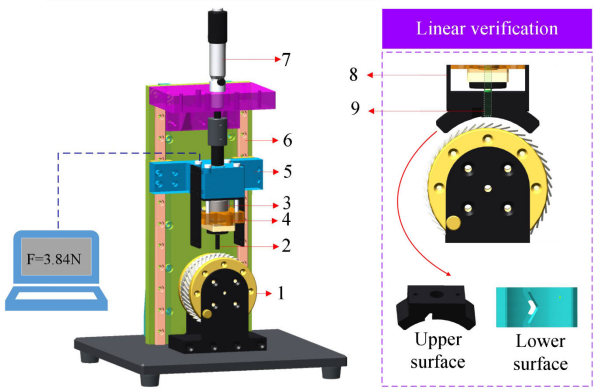

FIGURE 2. Mechanical performance testing platform.

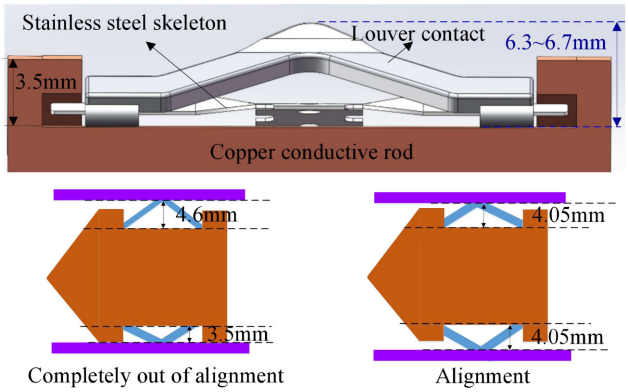

FIGURE 3. Louver contact connection structure.

pressure block and block supporter. During the experiment, the louver contact is fixed to the fixed end, the indenter is connected to the pressure sensor, the measurement range of the pressure sensor is 0∼30 N, and the fixture with the screw and nut to make the pressure sensor and the slider form a whole. During the experiment, the slider is moved on the slide by rotating the spiral micrometer so that the pressure sensor and the indenter compress the measured contact piece downward. The amount of compression of the contact piece is determined by the spiral micrometer, while the pressure on the contact piece is measured by the pressure sensor, and the force-compression mapping curve of a single contact piece during compression can be measured by the above device.

The pressure block and the block supporter in Fig. 2 in conjunction with the indenter can be used to simulate actual working conditions in which the louver contact pieces are subjected to pressure as a whole and to measure the force on a single contact piece under such conditions. The micrometer passes through a circular through-hole in the block supporter to contact the measured contact piece (the micrometer maintains the same curved surface as the lower surface of the pressure block). At the same time, the lower surface of the press block has a groove in the shape of a contact piece, which groove keeps the pressure block from contacting the measured contact piece, i.e., all the elastic force when the measured contact piece is pressed down is transferred to the indenter and measured by the pressure sensor. The pressure block is connected to the slider through the block supporter, i.e., the elastic force of the other contact pieces borne by the pressure block when it is pressed down is all carried by the slider, which does not affect the number of indications of the pressure sensor. By comparing the force-compression amount relationship of the contact pieces with and without the pressure block, it can be determined whether the force of the contact pieces is related to the compression state of its neighboring contact pieces.

B. FORCE-DEFORMATION MAPPING OF A SINGLE CONTACT PIECE

Fig. 3 shows the mating structure and dimensions of the louver contact with the plug and socket. When the louver contact is in a fully eccentric state (the outer wall of the plug fits the inner wall of the ferrule on one side), the maximum compression of the louver contact piece is 3.2mm, so the louver contact piece is compressed by 3.2mm during the measurement.

The pressure-compression mapping curves of the new monolithic contact pieces were measured and obtained using the mechanical property test platform without the pressure block, as shown in Fig. 4.

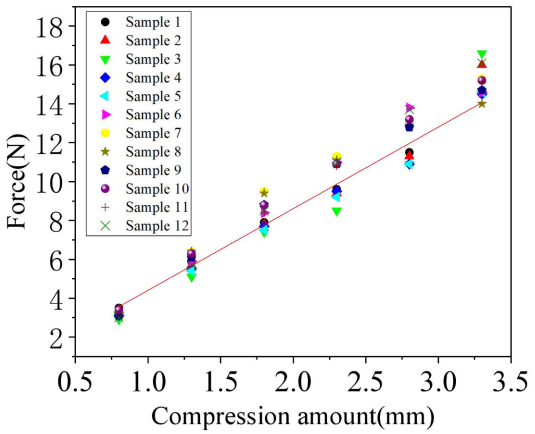

FIGURE 4. Mechanical performance testing platform.

It can be seen that the elastic force on the contact piece is close to a linear relationship with its compression, and the fitting equation between the two variables is:

$$F = 4.73x - 0.71 \tag{1}$$

where F/N is the elastic force applied to the contact piece and x/mm is the compression of the contact piece.

C. FORCE-CONTACT RESISTANCE MAPPING RELATIONSHIP

In this section, the contact resistance of the brand-new contact piece was further measured under different compression amounts, and the force-compression fitting expression was combined to obtain the force-contact resistance mapping

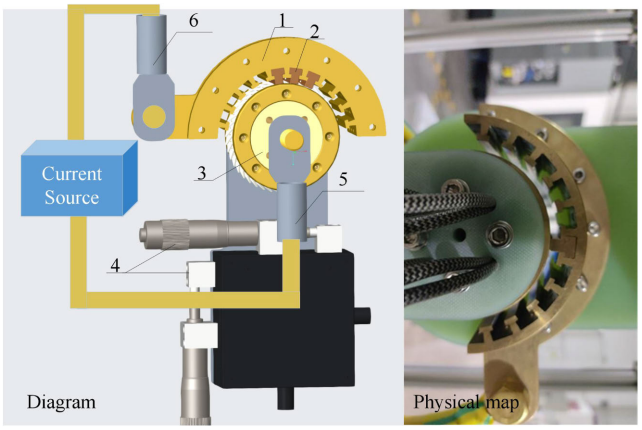

1:Pressure plate, 2: indenter, 3: Copper ring, 4: Micrometer, 5: Power supply anode hole, 6: Power supply cathode hole.

FIGURE 5. Device for measuring contact resistance.

relationship of the contact piece. The contact resistance measurement platform of the louver contact piece is shown in Fig. 5. Among them, the compression plate is completely fixed, and the number of compressed contact pieces is changed by embedding different numbers of indenters. The copper ring is used to place the experimental louver contact pieces. During the experiment, the compression amount of each contact piece on the strap as well as the eccentricity of the louver contact are adjusted by rotating two micrometers in different directions. The power supply anode and cathode are connected to the high-precision high-current generator, which can provide a DC ranging from 0 to 100 A to the measured contact piece.

Before the experiment, first embed a single piece of indenter and short the experimental circuit, the resistance (R_1) of the whole circuit is measured as 3.51 mΩ after the current is passed. After that, disconnect the power supply, fix the contact pieces of the brand-new strap on the copper ring, rotate the micrometer to compress the measured contact piece to the predetermined position, and then pass the current again and measure the resistance (R_2) of the circuit. It is necessary to explain that, to prevent the indenter from touching the other contact pieces, it is necessary to wrap the measured contact piece with insulating adhesive. It should be noted that to prevent the indenter from touching other contact pieces, the contact pieces under test should be wrapped with insulating gel. Finally, the measured resistance of the measured contact piece $R = R_2 - R_1$ (the value includes the contact resistance and volume resistance of the contact piece, but the volume resistance can be approximately ignored). Studies have shown that with the increase of contact current, the Joule heat generated by the contact resistance will reduce the hardness of the material, resulting in an increase in the number of contact spots and a decrease in the contact resistance [12]. Since the rated operating current of the converter transformer with excessive direct resistance is 3266 A, the three louver contacts are configured with 141 touch pieces, and the average rated operating current of each touch piece is 23 A. In addition to the peak holiday period, the flow will not run at full load. Therefore, in order to get close to the real operating conditions, this paper chooses the current condition of 20 A to measure the contact resistance of the louver contacts under different pressures. The measurement results of compression and contact resistance are shown in Fig. 6.

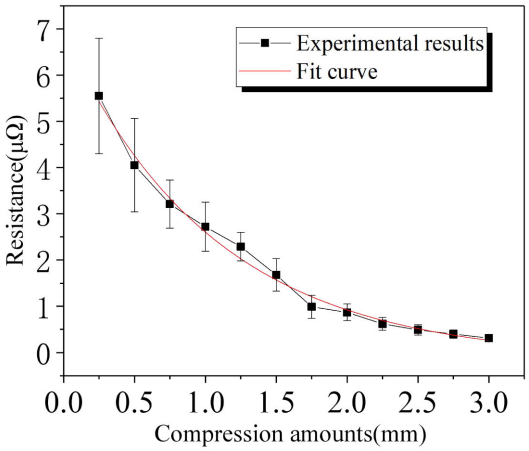

FIGURE 6. Relationship between resistance and compression.

It should be noted that the contact resistance measurements of the contact pieces reached stability only after one minute of current flow, and all the experimental data after 3 minutes of current flow are shown in Fig. 7. An exponential function was further used to fit the mapping relationship between force and compression, and the fitting equation was:

$$R = -0.158 - 7.064 * 0.391^{x} \quad (2)$$

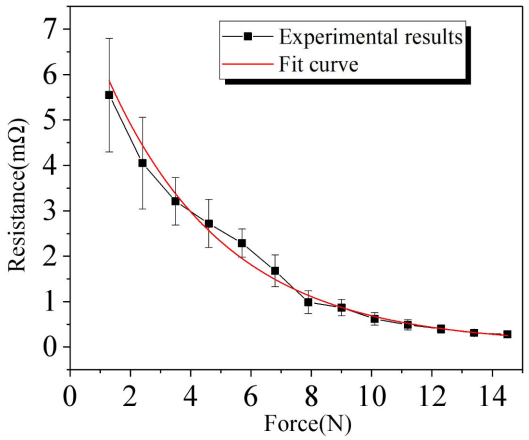

FIGURE 7. Relationship between resistance and force.

The R-squared of the fitted equation is 0.9932, which is a better fit. However, Eq. (2) can be used to calculate the contact resistance of the louver contact pieces only when the mapping relationship of force compression of the contact piece is kept constant. When the ambient temperature or the geometric parameters of the stainless steel skeleton are changed, Equations (1) and (2) are no longer applicable. Fortunately, since the silver-plated copper structure and material of the contact piece sheet are not changed in the study

of this paper, the mapping relationship between the elastic force and contact resistance of the contact piece sheet can be regarded as constant [13], [14], [15], and the compression in Fig. 6 is calculated as a force using Eq. (1), which is further fitted to obtain the mapping relationship of the force-contact resistance of the contact piece sheet as:

$$R = 7.38 * e^{(-0.23x)} \tag{3}$$

The R-squared of the fitted equation is 0.9913, which is a good fit.

III. MECHANICAL CALCULATION MODEL OF LOUVER CONTACTS

A. HYDROSTATIC MODEL CONTROL EQUATIONS

In this paper, the hydrostatic module of the Ansys workbench is used to simulate the force on the louver contact piece, and the governing equations of hydrostatics are as follows.

$$\begin{cases} \dfrac{\partial \sigma_{ij}}{\partial \mathrm{x}_j} + f_i = 0 \\ \varepsilon_{ij} = \dfrac{1}{2}\left(\dfrac{\partial u_i}{\partial x_j} + \dfrac{\partial u_j}{\partial x_i}\right) \\ \sigma_{ij} = C_{ijkl}\varepsilon_{kl} \end{cases} \tag{4}$$

where σ_{ij} is the stress tensor, f_{i} is the volumetric force, $\varepsilon_{\mathrm{ij}}$ is the strain tensor, u_{i} and u_{j} are the displacements in the i, j directions, respectively, and C_{ijkl} is the material elasticity tensor.

B. PARAMETERS OF THE MECHANICAL MODEL

The stainless steel keel of the louver contacts is made of 301EH spring steel, which is characterized by high hardness, high elasticity and high yield strength. In this paper, according to the standard requirements of GB/T 228.8-2015 [16], the samples were made and the stress-strain curves of this spring steel at different temperatures were measured, and the results are shown in Fig. 7.

Nitrogen protection was used in the test, the holding time was 15 minutes, and the deformation of the sample was measured using a mechanical extensometer. The measurement results in Fig. 8 show that the mechanical properties of stainless steel decrease as the ambient temperature increases, and when the ambient temperature reaches above 300 °C, the mechanical properties of spring steel deteriorate significantly.

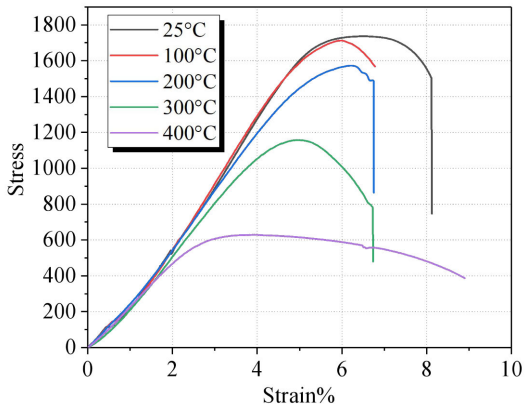

FIGURE 8. Stress-strain curve of stainless steel.

Since the yield point of stainless steel is not obvious, the modulus of elasticity and yield strength of spring steel at different temperatures are extracted by using $\sigma_{0.2}$ based on the stress-strain curve in Fig. 8, and the results are shown in Table 1.

TABLE 1. Mechanical parameters of 301EH stainless steel.

Temperature/°C	Young's modulus/GPa	Yield strength /MPa
25	41.6	1680
100	38.3	1660
200	36.9	1500
300	34.5	1100
400	32.3	580

For the silver-plated copper contacts, since the thickness of the silver-plated layer is only 50 μm, the effect of the silver plating is ignored, and the mechanical parameters of the silver-plated copper contacts are replaced by those of the purple copper, as shown in Table 2 [17].

TABLE 2. Mechanical parameters of contact finger.

Temperature/°C	Young's modulus/GPa	Yield strength /MPa
25	112.3	273.0
100	107.4	229.4
200	103.6	193.2
300	98.7	154.5
400	92.7	109.1

Based on the stress-strain curves, multilinear hardening curves were further selected in the statics module to describe the mechanical properties of the stainless steel keel and silver and copper-plated contact pieces after reaching the yield strength.

C. SIMPLIFICATION AND VALIDATION OF MECHANICAL MODELS

The compression process of the louver contacts has high geometric nonlinearity, material nonlinearity, and contact nonlinearity. Specifically, when the press block is pressed down, the contact plate and the stainless steel are twisted under pressure, resulting in a high geometric nonlinearity. The silver-plated copper contact and stainless steel keel may have plastic deformation during compression, and the nonlinear material is involved in the problem. In addition, the bottom of the contact piece and the electrical contact area also have relative slips with the plug and the socket, which is non-linear contact. The above phenomenon will increase the difficulty of the simulation model convergence, so it is necessary to simplify the mechanical model of the louver contacts reasonably to improve the convergence. The simplified model of this paper is formed by combining one, three and five

louver contacts with simplified steel strips. The simplified model of three louver contacts is taken as an example, and its physical structure and mesh division are shown in Fig. 9.

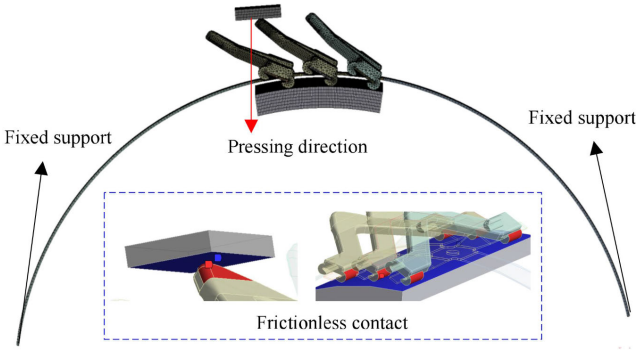

FIGURE 9. Model and mesh generation.

The contact between the contact piece and the pressure block and lower guide bar is set as frictionless contact in the model. At the same time, it is assumed that the ends of the stainless steel keel are kept stationary and set as fixed support. The compression block was moved down by 3.2 mm in the simulation to evaluate the force on the louver contacts under different compression amounts. To improve the calculation accuracy, the regular aggregates in the model (simplified steel belt, upper briquette and lower guide bar) are structured with structured meshes, and the meshes in each region are at least two layers.

When the compression of the contact piece reaches 3.2mm, the results of the VON-Mises equivalent force calculation of the louver contact in different simplified models are shown in Fig. 10. From this figure, it can be seen that when the contact piece is compressed, the stainless steel skeleton underneath it bears the main load, and these loads will be transferred to the two contact pieces immediately adjacent to it, i.e., the elastic force borne by a single contact piece under compression needs to be jointly supported with its immediately adjacent contact pieces. In addition, the maximum stress of the contact piece under pressure occurs in the middle region of the stainless steel belt in the torsion part and away from the pressure of the contact piece of the steel belt does not bear the stress.

A comparison of the calculated and experimentally measured force-compression of the monolithic contact piece in the three simplified models is shown in Fig. 11.

It can be seen that the computational error of the single-piece contact piece model exceeds 30%. Since the stress of the compressed contact piece can only be transmitted to its immediate neighboring contact pieces, the maximum error between the simulation results and the experimental results of the simplified models of the three-piece finger and the five-piece finger is no more than 15%. Therefore, under the premise of guaranteeing the accuracy of the calculation results and in order to save the calculation resources, the simplified model of three-piece contacts is used in the following.

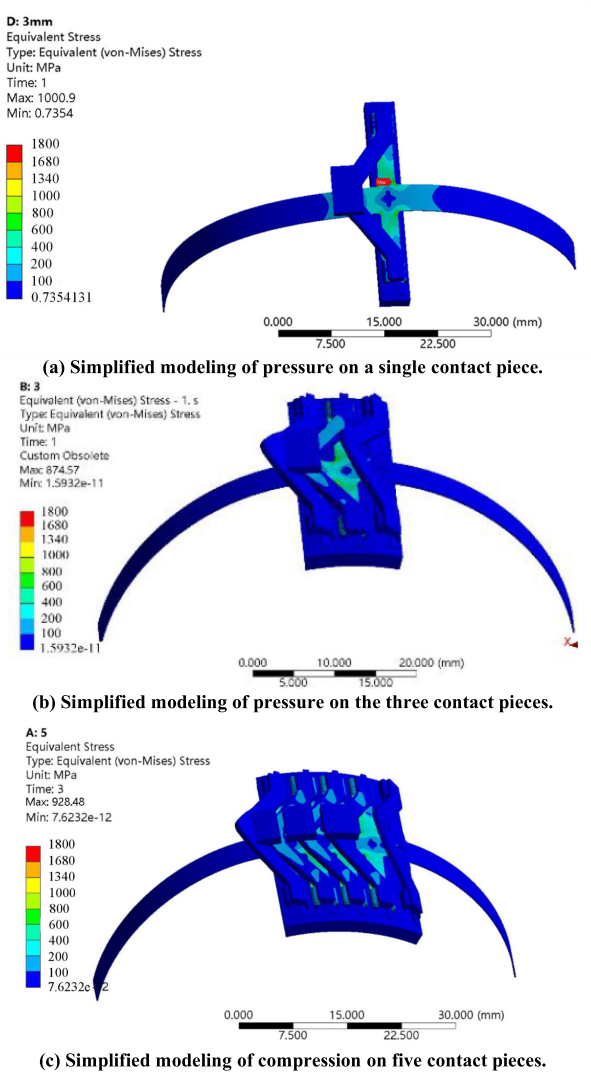

FIGURE 10. Comparison of simulation and experiment results.

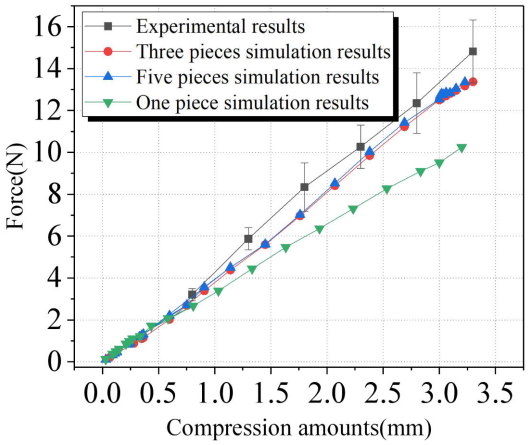

FIGURE 11. Comparison of simulation and experiment results.

D. EFFECT OF COEFFICIENT OF FRICTION

The calculated elastic force applied to the contact pieces in Fig. 10 is low compared to the measured results, which may

be caused by the use of frictionless contact in the model. The coefficient of friction between the contact pieces and the plug and socket is difficult to obtain accurately, but the coefficient of kinetic friction between copper and silver is usually in the range of 0.1 to 0.3. Therefore, the frictionless contact between the silver-plated copper contact pieces and the plug and socket in Fig. 9 was changed to a frictional contact and recalculated after setting the friction coefficients to 0.1, 0.2, and 0.3, respectively, to evaluate the effect of the friction coefficients on the calculation results. After setting different friction coefficients, the comparison of experimental and simulation results is shown in Fig. 12.

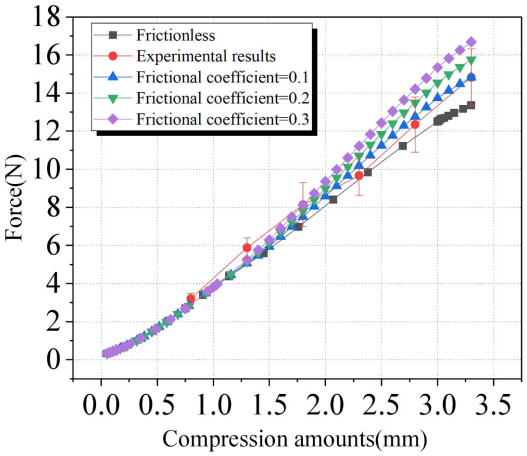

FIGURE 12. Comparison of simulation and experiment results,, after setting different friction coefficients.

It can be seen that the influence of the friction coefficient on the simulation results increases with the increase of the compression and elastic force. When the friction coefficient is 0.1, the experimental measurement results are closest to the calculated results, and the maximum deviation is only 7.43%. Therefore, the contact between the contact piece and the indenter and guide bar is set as frictional contact and the friction coefficient is set as 0.1 in the following simulations.

E. INDEPENDENCE OF FORCES ON THE CONTACT PIECES

Under the actual working conditions, the whole strap is compressed at the same time with more than forty contact pieces, and it is difficult to directly simulate the force of the whole strap due to the limitation of the calculation volume. However, if the force of each contact piece is independent of each other when the strap is compressed, the compression amount of each contact piece can be determined according to the relative position of the strap between the plug and the socket and the force-compression relationship in the simulation can be utilized to evaluate the force of each contact piece. Therefore, this section establishes a model for the simultaneous compression of multiple contact pieces. The model adopts the method of distributed calculation, specifically, the first compression of the contact piece B on the left side of the contact piece A, and then the compression of the contact piece C on the right side of the contact piece A. After keeping A and C in the state of compression, the contact piece A is pressed down again. if the force-compression curve of the contact piece A when pressed down is the same as that of the contact piece when pressed down individually in the above section, then it is proved that the force of the contact piece is independent of each other, and the results of the model calculations are shown in Fig. 13.

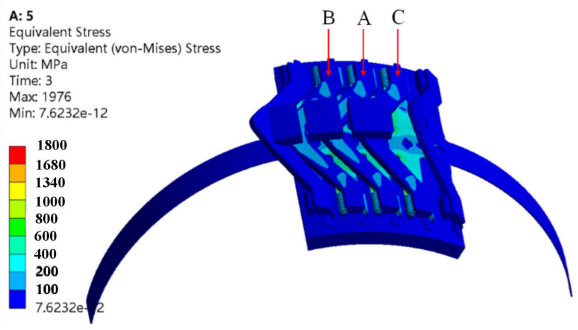

(a) Simulation results of simultaneous pressure on three contact pieces.

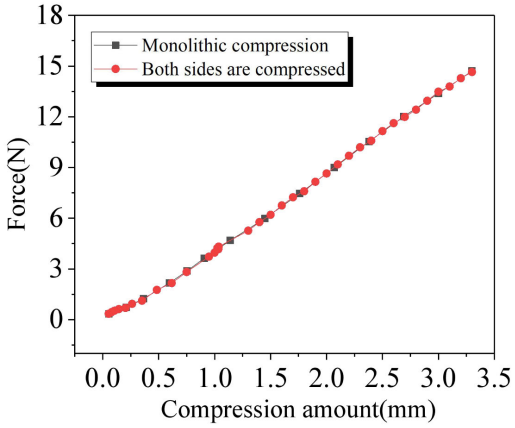

(b) Simulation results of simultaneous pressure on contacts with different numbers of pieces.

FIGURE 13. The independence of the force on contact pieces.

It can be seen that the forces on the contact pieces in the model are independent of each other. To further verify this viewpoint, the above mechanical properties of the contact piece test platform were loaded with a pressure block, and then the micrometer was turned again so that the tested contact piece and its neighboring contact pieces were compressed at the same time, and the force-compression measurements of a single piece of contact piece were compared with and without a pressure block, as shown in Fig. 14. It can be seen that the force-compression measurements of the contact pieces are also independent of the compression state of the neighboring contact pieces. Therefore, the forces on each contact piece are independent of each other when the strap is compressed.

Although the stresses on a single contact piece when compressed can be transferred to its immediate neighboring contact pieces, the narrow range and low relative value of the transferred stresses are the reason why the contact pieces are stressed independently of each other.

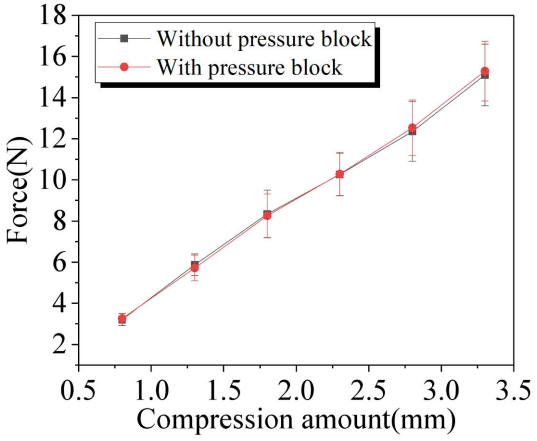

FIGURE 14. Comparison results of with or without pressure block.

F. MECHANICAL PROPERTIES OF LOUVER CONTACTS AT DIFFERENT TEMPERATURES

Experimental data on the stresses on the stainless steel keel of the strap under ambient temperature conditions, when the contact pieces are compressed by 3.2 mm, are shown in Fig. 15.

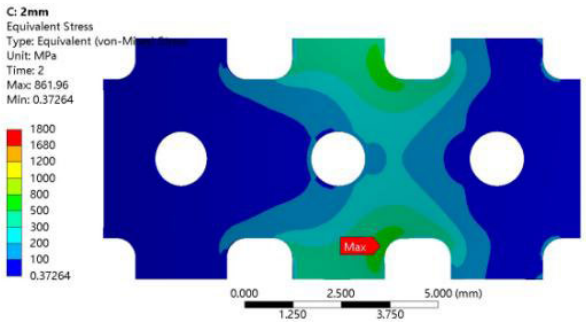

FIGURE 15. Comparison of simulation and experiment results.

It can be seen that the maximum stress borne by the stainless steel keel is 861.96 Mpa, which is much smaller than the yield strength, so no plastic deformation occurs in the louver contact under the ring temperature. Further, calculate the relationship curve between compression and force of louver contact under different temperatures, and the results are shown in Fig. 16.

As can be seen in Fig. 16, with the increase in temperature, the mechanical properties of the strap stainless steel decrease, the contact force of the contact piece under the same compression decreases, and the larger the compression, the more obvious the effect of temperature. The decrease in pressure causes the effective contact area between the contact piece and the current-carrying guide bar to decrease, and the contact resistance increases. Therefore, the localized heating of the louver contact will lead to a decrease in the contact force between the overheated contact piece and the plug and socket, and an increase in the contact resistance, resulting in a continued increase in the amount of heat generated by the overheated contact piece, which triggers corrosion and the

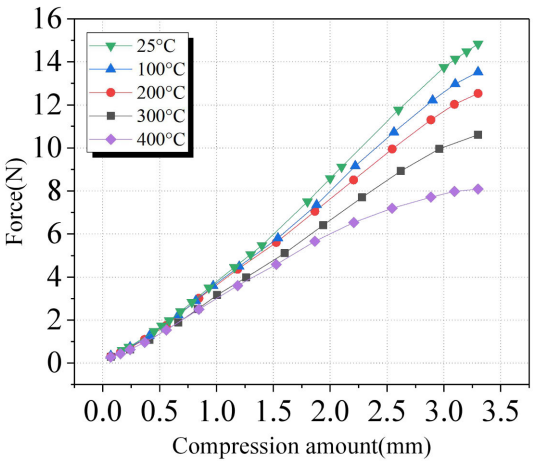

FIGURE 16. The influence of temperature.

formation of a vicious cycle. In different temperatures, the contact piece compression amount of 3.2 mm, the strap stainless steel keel withstand equivalent force shown in Fig. 17.

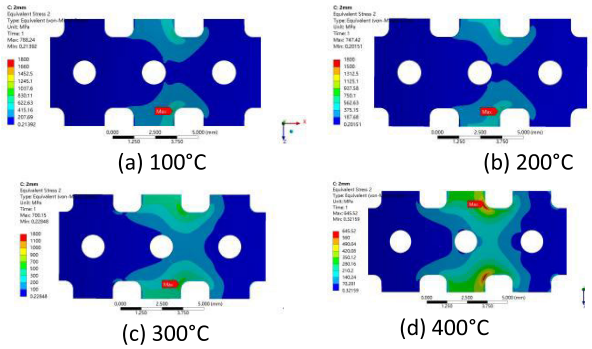

FIGURE 17. The independence of the force on the contact piece.

Therefore, the permanent plastic deformation of the contact piece occurs when the operating temperature of the stainless steel keel reaches 400 °C. The actual operating temperature of the louver contacts hardly reaches this temperature, i.e. the decrease in the mechanical properties of stainless steel at high temperatures is not the main reason for the plastic collapse of the louver contacts.

IV. OPTIMIZATION OF STAINLESS STEEL KEEL FOR STRAP

The thickness of the stainless steel of the strap and the degree of torsion of the ends affect the elastic force per unit of compression of the louver contacts as well as the compressibility of the louver contacts. In this section, the effects of the thickness and torsion angle of the stainless steel keel on the heating power of the louver contacts under fully eccentric conditions are investigated based on a simulation model. In this study, a single strap with a current of 1200 A and a total of 45 contact pieces on the strap had a current of 1200 A, and the temperature was set at 90 °C, the Structure of louver contacts is shown in Fig. 18.

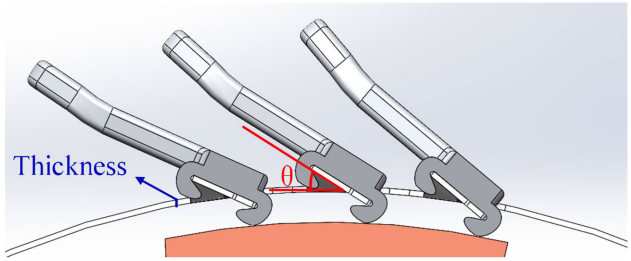

FIGURE 18. Structure of louver contacts.

The specific research methods are as follows: firstly, the force-compression curves of the contact pieces after changing the geometric parameters of stainless steel are calculated by using the mechanical simulation model. Then, the compression amount of each contact piece on the strap is calculated by combining the position and geometrical parameters of the plug, the sleeve and the stainless steel adjusted louver contact pieces under the condition of complete eccentricity, and the elastic force applied to each contact piece is obtained by interpolation based on the force-compression curve. The contact resistance R_i and its shunt I_i of contact piece i on the strap are calculated by combining the force-contact resistance mapping relationship of the contact piece obtained above, and finally, the heating power of each contact piece on the strap is solved by using the formula $P_i = I_i^2 R_i$.

A. INFLUENCE OF STEEL STRIP THICKNESS

The thickness of the stainless steel keel in the model was set to 0.15 mm, 0.2 mm (original thickness), 0.25 mm, and 0.3 mm, and the other physical structures remained unchanged. After changing the thickness of the stainless steel, the force-compression calculation results of the contact piece are shown in Fig. 19.

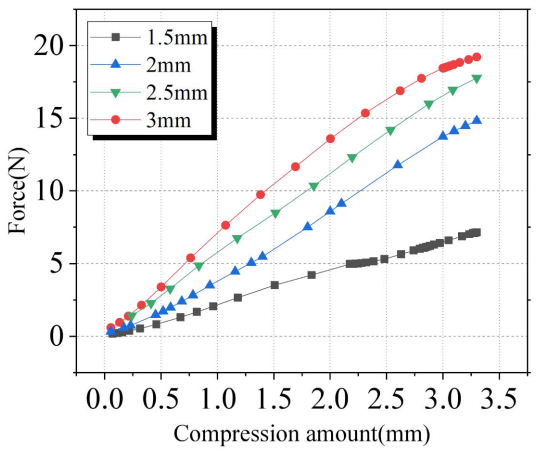

FIGURE 19. The influence of stainless steel thickness.

It can be seen that as the thickness of stainless steel increases, the slope of the force-compression curve due to compression of the contact piece increases. Further calculation of the heating power of the contact pieces of different thicknesses of stainless steel straps under fully eccentric conditions is shown in Fig. 20.

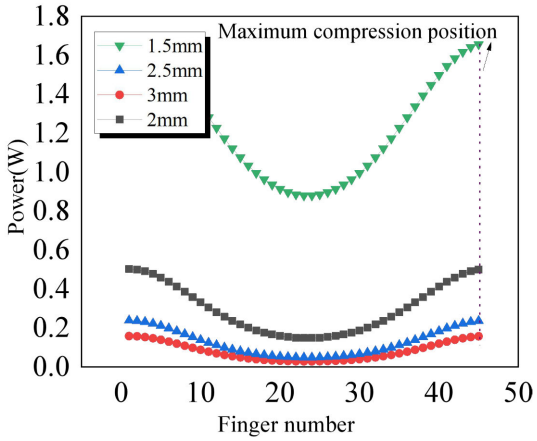

FIGURE 20. Distribution of heating power for the louver contacts.

As can be seen from Fig. 20, with the increase in stainless steel thickness, the contact pressure between the louver contact and the plug and sleeve increases, the contact resistance decreases, and the heating power decreases as a whole. From Fig. 7, it can be seen that with the increase in contact pressure, the contact resistance of the contact piece with the increase in pressure and the rate of decrease slows down, the phenomenon caused by the stainless steel thickness of the louver contact heating power with the increase in the thickness of the decrease. In addition, according to the settlement results in Fig. 20, it is easy to know that the thickness of the stainless steel of the strap should not be less than 2mm.

B. INFLUENCE OF TORSION ANGLE OF STAINLESS STEEL BELT

The torsion angles of the stainless steel were modified to 17°, 20.5°, 22° (original design), 24.5°, and 27°, and the maximum compressible amount of the contact pieces at each torsion angle was 2.70 mm, 2.89 mm, 3.20 mm, 3.56 mm, and 3.84 mm, respectively. The force-compression calculations of the contact pieces at different torsion angles are shown in Fig. 21.

It can be seen that as the torsion angle increases, the maximum compressibility of the contact piece increases, but the slope of the compression-elastic force curve remains constant. The effect of the stainless steel torsion angle on the heating power of the louver contact under eccentric conditions was further evaluated and the results are shown in Fig. 22.

The contact resistance of the contact pieces tends to stabilize with the increase of contact pressure. Therefore, with the increase of the torsion angle of the contact piece, the compression and elastic force of each contact piece on the strap increase, the contact resistance of the strap as a whole decreases and the distribution of the contact resistance under the condition of eccentricity becomes more uniform.

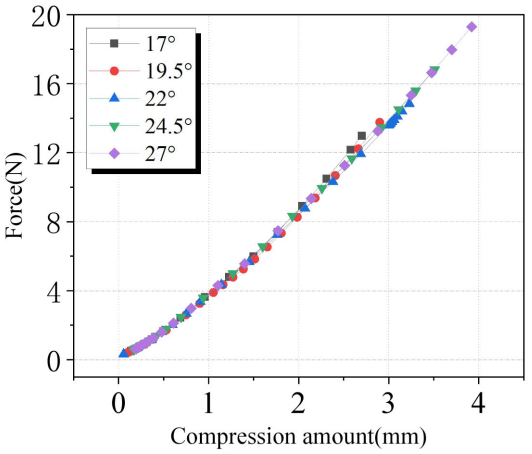

FIGURE 21. Force compression relationship at different angles.

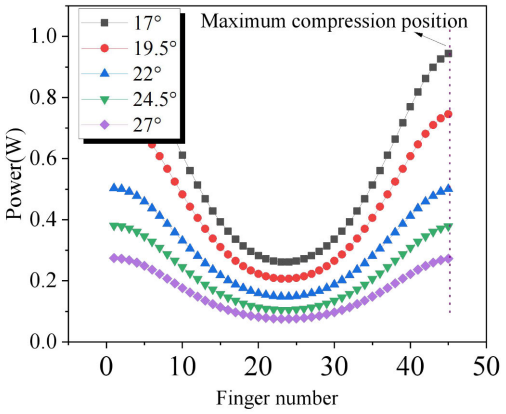

FIGURE 22. Distribution of heating power for the louver contacts.

In summary, the appropriate increase in the thickness and torsion angle of the stainless steel of the strap can reduce the overall heat generation of the contact pieces of the strap and slow down the local heat generation caused by the eccentricity.

V. DISCUSSION

There is a considerable number of plastic deformation of the louver contacts, and even if the strap is in an eccentric state and the surface of the louver contacts is corroded, the operating temperature of the strap is difficult to reach 400 °C. Therefore, the main reason for the plastic deformation of the louver contact is more likely to be the material change of stainless steel after long-term high-temperature service.

The preliminary metallogenetic test showed that the new spring had twin austenite and deformed martensite, while the degraded spring had twin austenite, deformed martensite and carbide precipitated phase. The new stainless steel band has an average Vickers hardness of 543, while the plastic deformation stainless steel band has an average Vickers hardness of 627. It is speculated that after higher service temperature, chromium-rich carbide precipitation in austenitic stainless steel increased the hardness of the old spring. With the precipitation of carbide, although its tensile strength and hardness will increase, its yield strength and elastic modulus will be significantly reduced [15]. The above phenomenon may be an important reason for the plastic deformation of the louver contacts, and the research team will conduct in-depth research on this phenomenon in the next step.

VI. CONCLUSION

Based on the performance test platform of oil-immersed louver contact pieces, this paper obtains the mapping relationship between force-compression and force-contact resistance of oil-immersed louver contacts, establishes the mechanical simulation model of louver contacts, and investigates the influence of plastic deformation temperature of louver contacts and geometric parameter of stainless steel on the heating power of louver contacts. The research results are helpful to understand the mechanism of local overheating failure of oil-immersed electric contact parts, and provide a reference for the design, fault analysis and further research of oil-immersed electric contact parts. And the conclusions are as follows:

(1) The elastic force on the contact piece and its compression amount satisfy the linear relationship, and the force on each contact piece on the strap is independent of each other.

(2) The elastic force on the contact piece and its contact resistance satisfy the power function relationship.

(3) the mechanical properties of the contact piece decrease with the increase in temperature, and the plastic deformation of the contact piece occurs when the temperature reaches 400 °C. The mechanical properties of the contact piece decrease with the increase of temperature.

(4) Appropriately increasing the thickness and torsion angle of the stainless steel of the strap can reduce the overall heat generation of the strap's contact piece and slow down the local heat generation problem caused by the eccentricity of the link.

APPENDIX

In order to make it easier for the reader to understand this article, all the symbols that appear in this paper are shown in Table 3 in the appendix.

TABLE 3. List of symbols used in this paper.

Symbol	Quantity
F / N	Elastic force applied to the contact piece
x / mm	The compression of the contact piece
σ_{ij}	Stress tensor
f_i	Volumetric forcet
ε_{ij}	Strain tensor
u_i	Displacements in the i directions
u_j	Displacements in the j directions
C_{ijkl}	Material elasticity tensor
R_1	Whole circuit resistance embedded in a single indenter
R_2	Loop resistance
R	Resistance of the measured contact piece

REFERENCES

[1] H. Duan, "Cause analysis of abnormal resistance of electrical contact elements in the UHV value side ascending flange," *Power Grid. Technol.*, 2023.
[2] Z. Liu and Q. Zhang, "Study on the development mode of national power grid of China," *Proc. CSEE*, vol. 33, no. 7, pp. 1–10, 2013.
[3] S. Zhang and Z. Peng, "Design and analysis of insulation structure of ±800-kV valve side converter transformer bushing," *High Voltage Eng.*, vol. 45, no. 7, pp. 2257–2266, 2019.
[4] H. Tian, S. Jin, A. Gong, Z. H. Wu, Q. Y. Wang, P. Liu, and Z. Peng, "Analysis on the deterioration behavior of electrical contact structure used in converter transformer RIP bushings," *Proc. CSEE*, vol. 41, no. 3, pp. 1146–1156, 2021.
[5] A. Zhou, L. Gao, X. Ji, M. Zhang, and H. Tang, "Analysis and field-repair of current overheating faults on dry type SF_6 gas-insulated valve side bushing in converter transformer," *Power Grid Technol.*, vol. 42, no. 5, pp. 1401–1409, 2018.
[6] H. Tang, G. Wu, J. Deng, M. Chen, X. Li, and K. Liu, "Electro-thermal comprehensive analysis method for defective bushings in HVDC converter transformer valve-side under multiple-frequency voltage and current harmonics," *Int. J. Electr. Power Energy Syst.*, vol. 130, Sep. 2021, Art. no. 106777.
[7] M. Gatzsche, N. Lucke, S. Großmann, T. Kufner, B. Hagen, and G. Freudiger, "Electric-thermal performance of contact elements in high power plug-in connections," in *Proc. IEEE 60th Holm Conf. Electr. Contacts (Holm)*, Oct. 2014, pp. 1–8.
[8] M. Gatzsche, N. Lucke, S. Großmann, T. Kufner, and G. Freudiger, "Evaluation of electric-thermal performance of high-power contact systems with the voltage-temperature relation," *IEEE Trans. Compon., Packag., Manuf. Technol.*, vol. 7, no. 3, pp. 317–328, Mar. 2017.
[9] S. Jin, H. Tian, Q. Wang, T. Ren, P. Liu, and Z. Peng, "Corrosion reaction kinetics and high-temperature corrosion testing of contact element strips in ultra-high voltage bushing based on the phase-field method," *IET Gener. Transm. Distrib.*, vol. 16, no. 15, pp. 2947–2958, 2022.
[10] S. Jin, "Overheating corrosion characteristics of current carrying connection structure of ultrahigh voltage gas insulated transmission equipment," *Power Grid Technol.*, pp. 1–9, 2022.
[11] W. Yang, "Research on current carrying wear characteristics and analysis of electrical contact performance degradation of high voltage GIS equipment plug structures," *J. Tribol.*, 2023.
[12] F. Guo and Z. Chen, *Electric Contact Theory and Appliedtechnology*. Beijing, China: China Electric Power Press, 2008.
[13] G. Slade, *Electrical Contacts Principles and Applications*. New York, NY, USA: Marcel Dekker, 1999.
[14] P. Liu, "Numerical calculation of contact resistance of sleeve watchband on rheological valve side," *High Voltage Eng.*, vol. 49, no. 3, pp. 1184–1193, 2023.
[15] *State Administration of Quality Supervision, Inspection and Quarantine*, GB/T 228.8-2015, Tensile Test of Metal Materials, Standards Press of China, Beijing, China, 2011.
[16] P. Ogar, E. Ugryumova, and I. Koryakyn, "The influence of the mechanical properties of copper at elevated temperatures on the tightness of the sealing joint," *Mater. Today, Proc.*, vol. 38, pp. 1764–1768, Jan. 2021.
[17] Z. Wang, *Effect of SMAT on Microstructure and Mechanical Properties of AISI301 Stainless Steel After Cryogenic Treatment*. Nanchang, China: Nanchang Univ., 2017.

ZHICHENG HUANG was born in Henan, China, in 1993. He received the Ph.D. degree from North China Electric Power University, Beijing, China, in 2022. He is currently an Engineer with State Grid Sichuan Electric Power Research Institute. His research interests include insulation structure optimization design of power equipment, multi-physics field simulation, and electrical contact characteristics.

FAN LIU was born in Chongqing, China, in 1978. He received the Ph.D. degree from Chongqing University, Chongqing, China. His research interest includes online monitoring of electrical equipment.

YANMING TU was born in China, in 1972. He received the master's degree from Xi'an Jiaotong University. He is currently a Senior Engineer with State Grid Sichuan Electric Power Research Institute. His research interests include metal materials, processes, and devices for power grid equipment.

JIAHUI CHEN was born in China, in 1991. She received the Ph.D. degree from Tsinghua University, in 2018. She is currently a Senior Engineer with State Grid Sichuan Electric Power Research Institute. Her research interests include metal materials, processes, and devices for power grid equipment.

SHIHONG HU was born in China, in 1975. She is currently a Senior Engineer with the Electric Power Science Research Institute, State Grid Sichuan Electric Power Research Institute. Her research interests include transformer insulation oil and transformer fault diagnosis.

TAO ZHAO (Member, IEEE) was born in Baoding, Hebei, China, in 1982. He received the B.Eng. degree from North China Electric Power University, in 2005, the M.Sc. degree from Chongqing University, in 2008, and the Ph.D. degree from North China Electric Power University, in 2017. His research interests include the insulation monitoring of power transformers and fault detection and diagnosis of electric equipment.

YUNPENG LIU (Member, IEEE) was born in Anhui, China, in 1976. He received the B.Eng. and Ph.D. degrees in electrical engineering from North China Electric Power University, Baoding, China, in 1999 and 2005, respectively. He is currently a Ph.D. Supervisor and a Professor with North China Electric Power University. His research interests include UHV transmission, fault detection, and diagnosis of electric equipment.